

Mini Black Holes at the LHC

Discovery Through Di-Jet Suppression, Mono-Jet Emission and a Supersonic Boom in the Quark-Gluon Plasma in ALICE, ATLAS and CMS

B. Betz², M. Bleicher², U. Harbach¹, T. Humanic³, B. Koch^{1,2}, H. Stöcker^{1,2}

¹ FIAS- Frankfurt Institute for Advanced Studies

D-60438 Frankfurt am Main, Germany

² Institut für Theoretische Physik, Johann Wolfgang Goethe - Universität

D-60438 Frankfurt am Main, Germany

³ Department of Physics

Ohio State University, Columbus, OH, USA

Abstract. We examine experimental signatures of TeV-mass black hole formation in heavy ion collisions at the LHC. We find that the black hole production results in a complete disappearance of all very high p_T (> 500 GeV) back-to-back correlated di-jets of total mass $M > M_f \sim 1\text{TeV}$. We show that the subsequent Hawking-decay produces multiple hard mono-jets and discuss their detection. We study the possibility of cold black hole remnant (BHR) formation of mass $\sim M_f$ and the experimental distinguishability of scenarios with BHRs and those with complete black hole decay. Finally we point out that a Heckler-Kapusta-Hawking plasma may form from the emitted mono-jets. In this context we present new simulation data of Mach shocks and of the evolution of initial conditions until the freeze-out.

Keywords: LHC, black holes

PACS: specifications see, e.g. <http://www.aip.org/pacs/>

1. Introduction

The Frankfurt-born astronomer Karl Schwarzschild discovered the first analytic solution of the General Theory of Relativity [1]. He laid the ground for studies of some of the most fascinating and mysterious objects in the universe: the black holes. Recently, it was conjectured that black holes (BH) do also reach into the regime of particle and collider physics: In the presence of additional compactified large extra dimensions (LXDs), it seems possible to produce tiny black holes in

colliders such as the Large Hadron Collider (LHC), at the European Center for Nuclear Research, CERN. This would allow for tests of Planck-scale physics and of the onset of quantum gravity - in the laboratory! Understanding black hole physics is a key to the phenomenology of these new effects beyond the Standard Model (SM).

During the last decade, several models [2, 3, 4] using extra dimensions as an additional assumption to the quantum field theories of the Standard Model (SM) have been proposed. The most intriguing feature of these models is that they provide a solution to the so-called hierarchy problem by identifying the "observed" huge Planck-scale as a geometrical feature of the space-time, while the true fundamental scale of gravity M_f may be as low as 1 TeV. The setup of these effective models is partly motivated by String Theory. The question whether our space-time has additional dimensions is well-founded on its own and worth the effort of examination.

In our further discussion, we use the model proposed by Arkani-Hamed, Dimopoulos and Dvali [3], proposing d extra spacelike dimensions without curvature, each of them compactified to a certain radius R . Here all SM particles are confined to our 3+1-dimensional brane, while gravitons are allowed to propagate freely in the (3+d)+1-dimensional bulk. The Planck mass m_{Pl} and the fundamental mass M_f are related by

$$m_{Pl}^2 = M_f^{d+2} R^d \quad . \quad (1)$$

The radius R of these extra dimensions can be estimated using Eq.(1). For d equaling 2 to 7 and $M_f \sim \text{TeV}$, R extends from 2 mm to ~ 10 fm. Therefore, the inverse compactification radius $1/R$ lies in energy range eV to MeV, respectively. The case $d = 1$ is excluded: It would result in an extra dimension about the size of the solar system. For recent updates on constraints on the parameters d and M_f see e.g. Ref. [5].

2. Estimates of LXD-black hole formation cross sections at the LHC

The most exciting signature of LXDs is the possibility of black hole production in colliders [6, 7, 8, 9, 10, 11, 12, 13, 14, 15, 16, 17, 18, 19, 20, 21, 22, 23, 24, 25] and in ultra high energetic cosmic ray events [26, 27]: At distances below the size of the extra dimensions the Schwarzschild radius [28] is given by

$$R_H^{d+1} = \frac{2}{d+1} \left(\frac{1}{M_f} \right)^{d+1} \frac{M}{M_f} \quad . \quad (2)$$

This radius is much larger than the corresponding radius in 3+1 dimensions. Accordingly, the impact parameter at which colliding particles form a black hole via the Hoop conjecture [29] rises enormously in the extra-dimensional setup. The

LXD-black hole production cross section can be approximated by the classical geometric cross section

$$\sigma(M) \approx \pi R_H^2 \quad , \quad (3)$$

which only contains the fundamental scale as a coupling constant.

This classical cross section has been under debate [30, 31, 32]: Semi-classical considerations yield form factors of order one [33], which take into account that only a fraction of the initial energy can be captured behind the Schwarzschild-horizon. Angular momentum considerations change the results by a factor of two [34]. Nevertheless, the naive classical result remains valid also in String Theory [35].

Stronger modifications to the BH cross section are expected from recent calculations introducing a minimal length scale, suggested by String Theory and Loop Quantum Gravity alike. Via the use of a model implementing a Generalized Uncertainty Principle (GUP), one can show that a minimal length scale leads to a reduction of the density of states in momentum space at high energies. The squeezing of the momentum states not only reduces the black hole cross section, but also Standard Model cross sections involving high momentum transfer [21], see Fig. 1.

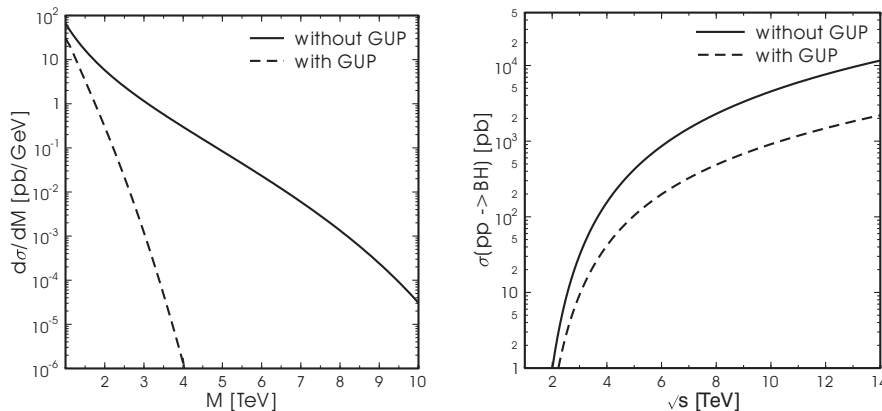


Fig. 1. The left plot shows the differential cross section for black hole production in p-p collisions at $\sqrt{s} = 14\text{TeV}$ (LHC) for $M_f = 1\text{ TeV}$. The right plot shows the integrated cross section for BH production as a function of the collision energy \sqrt{s} . In both cases, the curves for various d differ only slightly from the above depicted ones. The dashed curves show calculations including the minimal length (via a Generalized Uncertainty Principle (GUP)) [21, 22].

Setting $M_f \sim 1\text{ TeV}$ and $d = 2-7$ one finds cross-sections of $\sigma \sim 400\text{ pb}-10\text{ nb}$. Using the geometrical cross section formula, it is now possible to compute the differential cross section $d\sigma/dM$ for p-p collisions with an invariant energy \sqrt{s} . This cross section is given by the summation over all possible parton interactions and

integration over the momentum fractions x_i , where the kinematic relation $x_1 x_2 s = \hat{s} = M^2$ has to be fulfilled. This yields the expression

$$\frac{d\sigma}{dM} = \sum_{A,B} \int_0^1 dx_1 \frac{2\sqrt{\hat{s}}}{x_1 s} f_A(x_1, \hat{s}) f_B(x_2, \hat{s}) \sigma(M, d). \quad (4)$$

A numerical evaluation [22] using the CTEQ4-parton distributions $f_i(x, Q)$ results in the cross section displayed in Figure 1.

One can see that independent of the specific scenario, most of the black holes created have masses close to the production threshold. This is due to the fact that the parton distribution functions $f_i(x_i)$ are strongly peaked at small values of the momentum fractions x_i .

At the LHC up to 10^9 black holes may be created per year with the estimated full LHC luminosity of $L = 10^{34} \text{cm}^{-2} \text{s}^{-1}$ at $\sqrt{s} = 14$ TeV: Depending on the specific scenario, about ten black holes per second could be created [7]. LXD-black hole production would have dramatic consequences for future collider physics: Once the collision energy crosses the threshold for black hole production, no further information about the structure of matter at small scales can be extracted - this would be "the end of short distance physics" [9].

3. Suppression of high mass correlated di-jet signals in heavy ion collisions

The above findings led to a high number of publications on the topic of TeV-mass black holes at colliders [7, 8, 9, 10, 11, 17, 19, 20, 23, 24, 36, 37, 39, 41, 47, 48, 49, 51, 52], for hadronic collisions as well as for heavy ion collisions [19, 23, 38]: At the same center of mass energy, the number of black holes in a heavy ion event compared to a hadronic event is increased by about thousandfold due to the scaling with the number of binary collisions [38]. We will discuss special features of heavy ion collisions in Sec. 7.

The first, cleanest signal for LXD-black hole formation in Pb-Pb collisions is the complete suppression of high energy back-to-back-correlated di-jets with $M > M_f$: two very high energy partons which usually define the di-jets in the Standard Model, each having an energy of \sim one-half M_f (i.e. $p_T \geq 500$ GeV), now end up inside the black hole [19, 20, 23, 39] instead of being observable in the detector. Di-jets with $E_{di-jet} > M_f$ cannot be emitted.

4. Hard, isotropic multiple mono-jet emission as a signal for hot LXD-black hole hawking-evaporation

Once produced, the black holes may undergo an evaporation process [40] whose thermal properties carry information about the parameters M_f and d . An analysis of the evaporation will therefore offer the possibility to extract knowledge about the topology of space time and the underlying theory.

The evaporation process can be categorized in three characteristic stages [9, 11, 41]:

1. **BALDING PHASE:** In this phase the black hole radiates away the multipole moments it has inherited from the initial configuration and settles down in a hairless state. During this stage, a certain fraction of the initial mass will be lost in gravitational radiation.
2. **EVAPORATION PHASE:** The evaporation phase starts with a spin down phase in which the Hawking radiation carries away the angular momentum, after which it proceeds with emission of thermally distributed quanta until the black hole reaches Planck mass. The radiation spectrum contains all Standard Model (and possibly SUSY-) particles, which are emitted on our brane, as well as gravitons, which may also propagate into the extra dimensions as well. It is expected that most of the initial energy is emitted during this phase into Standard Model particles. A very thorough description of these evaporation characteristics has been given in [42].
3. **PLANCK PHASE:** Once the black hole has reached a mass close to the Planck mass, it falls into the regime of quantum gravity and predictions become increasingly difficult. It is generally assumed that the black hole will then either completely decay in a few Standard Model particles or form a quasi-stable remnant.

To understand the signature caused by black hole decay, we have to examine the Hawking evaporation process in detail: The evaporation rate dM/dt can be computed for an arbitrary number of dimensions using the thermodynamics of black holes. The Hawking-temperature (T) depends on the black hole radius

$$T = \frac{1+d}{4\pi} \frac{1}{R_H} \quad , \quad (5)$$

which is given by Eq. (2). The smaller the black hole, the larger its temperature.

Integrating the thermodynamic identity $dS/dM = 1/T$ over M yields the entropy

$$S(M) = 2\pi \frac{d+1}{d+2} (M_f R_H)^{d+2} \quad . \quad (6)$$

With rising temperature, the emission of a particle will have a non-negligible influence on the total energy of the black hole. This problem can appropriately be addressed by including the back-reaction of the emitted quanta as derived in Ref. [43, 44]. It is found that in the regime of interest, when M is of order M_f , the number density for a single particle micro state $n(\omega)$ is modified and now given by the change of the black hole's entropy:

$$n(\omega) = \frac{\exp[S(M-\omega)]}{\exp[S(M)]} \quad . \quad (7)$$

From this, using the evaporation rate we obtain

$$\frac{dM}{dt} = \frac{\Omega_{(3)}^2}{(2\pi)^3} R_H^2 \int_0^M \frac{\omega^3 d\omega}{\exp[S(M-\omega) - S(M)]} , \quad (8)$$

where $\Omega_{(3)}$ is the 3-dimensional unit sphere. Fig. 2 shows this rate as a function of M for various d . One observes that the evaporation process of the black holes slows down in its late stages [11, 12] ¹, and may even come to a complete stop, thus, stable black hole remnants may be formed [12, 23, 24, 45, 52].

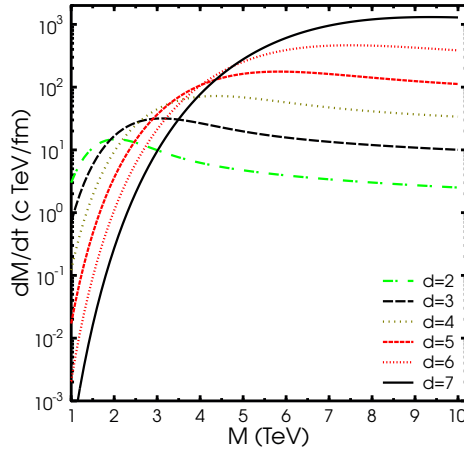


Fig. 2. The Black hole evaporation rates as a function of the initial black hole mass for various d [11].

The above discussion allows for the following observations:

- Typical temperatures for LXD-black holes with $M_{BH} \gg M_f$, e.g. 5 – 10 TeV, are several hundred GeV. This high temperature results in a very short lifetime. The black hole will decay close to the primary interaction region and thus its decay products can be observed in collider detectors.
- Most of the SM particles of the black body radiation are emitted with ~ 100 GeV average energy, which leads to multiple high energy mono-jets with much higher multiplicity than in Standard Model processes [23].
- The total number of emitted jets can be estimated to be of order 10. Because of the thermal characteristics of the decay, the pattern will be nearly isotropic, with a high sphericity of the event.

¹In a 3-dimensional theory this enhanced lifetime can also be obtained from a renormalization group approach [45].

Ideally, the energy distribution of the decay products allows for a determination of the temperature (by fitting the energy spectrum to the predicted shape) as well as of the total mass of the BH (by summing up all energies). This then will allow for a reconstruction of the fundamental scale M_f and the number of extra dimensions.

Several experimental groups have included LXD-black hole searches into their research programs for physics beyond the Standard Model, in particular the ALICE, ATLAS and CMS collaborations at the LHC [47]. PYTHIA 6.2 [48] with the CHARYBDIS [49] event generator allows for a simulation of black hole events and data reconstruction from the decay products. Such analysis has been summarized in Refs. [47, 50, 51].

5. Formation of stable black hole remnants and single track detection in the ALICE-TPC

To obtain predictions for collider experiments, one has to produce numerical simulations incorporating black hole events. These simulations have been performed but have so far assumed mostly that the black holes decay completely into Standard Model particles. As already pointed out, however, there are equally strong indications that the black holes do NOT evaporate completely, but rather leave a meta-stable black hole remnant (BHR) [11, 12, 13, 23, 24, 45, 52].

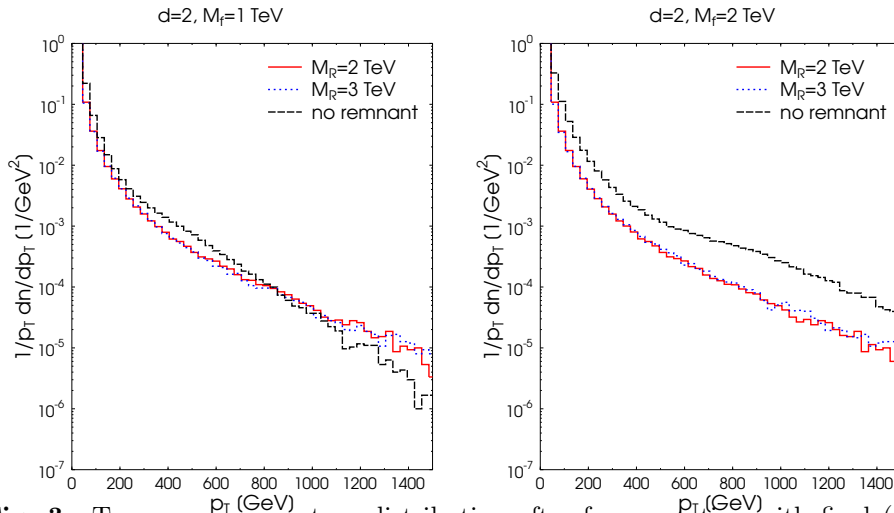


Fig. 3. Transverse momentum distribution after fragmentation with final (two-body) decay in contrast to the formation of a black hole remnant [52]

Figure 3 shows the p_T -spectra after fragmentation for complete black hole decay as well as for remnant formation for p-p collisions at the LHC. The spectra have been obtained with the CHARYBDIS simulation [49] and the observables computed

within the PYTHIA framework. It is apparent that the additional contribution from the final decay causes a clear difference between the curves with/without remnant formation. The BHR signal is thus clearly distinguishable from disappearing black holes.² These results also agree very well with analytically computed results [52].

If BHRs are formed, they can carry charge and may thus not only be reconstructed via decay products, but can rather directly be observed: Charged BHRs should appear in the ALICE detector at the LHC as a magnetically very stiff charged (small curvature) track. As shown in Fig. 4, the mass of a charged BHR can be reconstructed within the ALICE time of flight and spatial resolution [47].

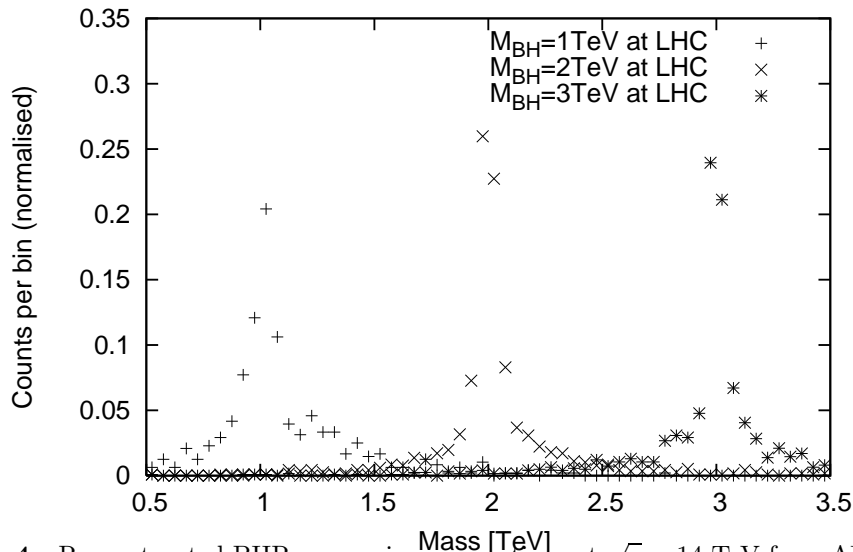


Fig. 4. Reconstructed BHR masses in p-p reactions at $\sqrt{s} = 14$ TeV from ALICE (TOF 56 ps) resolution for $M_{\text{BH}} = 1, 2, 3$ TeV.

6. Heckler-Kapusta-Hawking plasma and hard mono-jet suppression

The energy density of the multiple Hawking mono-jets emitted from the evaporating black holes is enormous: Several TeV are emitted within a 4-sphere of $\sim (10^{-1})^4 - (10^{-2})^4 \text{ fm}^4/c$, implying energy densities of 10^6 to 10^9 GeV fm^{-3} , i.e. many orders of magnitude higher than the energy densities expected for the quark-gluon plasma ($\epsilon \sim 500 \text{ GeV fm}^{-3}$) which is expected to be created in Pb-Pb collisions at the LHC at $\sqrt{s_{NN}} = 5.5 \text{ TeV}$ [23].

²The graph does not include background, but detectors like ALICE can differentiate LXJ-black holes from the QCD background [47, 53].

Hence, the question arises whether the multiple jets thermalize at this enormous energy density and form an ultra-hot ($T \gg T_{EW} \gg T_{QCD}$) plasma of Standard Model- (plus SUSY-)particles.

Such a hot Heckler-Kapusta-Hawking (HKH) plasma-scenario for primordial 3+1-dimensional black holes which could now decay and show up in cosmic radiation components has been studied by Heckler, Kapusta and co-workers [54, 55]. For the LXD-black holes and BHRs to be created in p-p reactions at the LHC, a similar plasma might be produced [10]: Such a HKH plasma at $T \sim 1$ TeV should contain many massless SM particles, as T is above the electroweak phase transition temperature [23, 24]. The bare masses of e.g. $W^{+/-}$ and Z as well as light supersymmetric partners may thus become accessible to experiment. Further interesting topics to study in this context include thermalization and viscosity of this SM-SUSY state of matter, hydrodynamic expansion, abundant pre-hadronic freeze-out emission of (otherwise rare) SUSY particles, quarks (b, t) and leptons [23, 24].

After formation, the HKH plasma will expand rapidly according to the relativistic viscous hydrodynamic transport equations [56]. In the ideal fluid approximation, this three-dimensional radial expansion can be approximated by the simple relativistic blast wave model [57, 58], which describes the particle spectra

$$\frac{d^3\sigma}{dp^3} = N \exp(-\gamma E/T) \left[\left(\gamma + \frac{T}{E} \right) \frac{\sinh \alpha}{\alpha} - \frac{T}{E} \cosh \alpha \right] \quad , \quad (9)$$

after a common hydrodynamic isentropic expansion freezing out with a common freeze-out temperature $T_{f.o.}$, and a common collective freeze-out velocity $v_{f.o.}$ ³

The nearly isentropic radial expansion causes strong space-momentum correlations, resulting in a spherical shell of "cool" (i.e. $T = 150$ MeV) hadronic matter at the hadronic freeze-out. Nearly all initial thermal energy is then transformed into collective radial motion, i.e. the mean flow velocity v_F is close to the speed of light. Hence, the invariant p_T spectra of hadrons exhibit peaks at the $p_T = 100$ GeV range. The residual hadronization temperature of $T = 150$ MeV in the rest frame of the fluid causes small thermal smearing in the spectra. We see that the final spectra seen in the HKH plasma scenario will appear quite differently than the shoulder-arm spectra in heavy ion collisions, which exhibit moderate flow velocities of $v_F = 0.5 c$.

7. Black holes created in heavy ion collisions: What are the interactions of BHR, the hot HKH plasma and of Hawking-radiation jets with the quark-gluon plasma created in Pb-Pb at the LHC?

In p-p collisions, the above discussed HKH fluid expansion and/or Hawking-radiation jet-emission will take place in the vacuum. In heavy ion collisions, black holes cre-

³Here, $\gamma = (1 - v_{f.o.}^2)^{-1/2}$, $\alpha = \gamma v_{f.o.} p/T$ and N gives an absolute normalization.

ated in individual parton-parton collisions will create the hot HKH fluid, which expands **”into”** the surrounding – much cooler – QCD plasma which has been created by soft parton collisions of up to 400 participating nucleons with an initial temperature of $T \sim 500$ MeV, i.e. about 1/1000-th of the Black Hole plasma temperature, $T \sim 500$ GeV. The extremely high energy density in the HKH plasma can cause shock discontinuities, travelling as nonlinear high density shock waves through the quark-gluon plasma. This phenomenon is quite analogous to the shock fronts discussed in heavy ion collisions since three decades [59, 60, 61].

A recent interesting speculation about the fate of hard jets emitted from the hard parton-parton collisions in Pb-Pb reactions (both at RHIC and LHC) has been the prediction of Mach-shock cones, plasma wakes or, respectively, curved Mach shock waves, excited in the dense medium by the propagating jets [23, 60, 61, 62].

The properties of the matter in front and behind such shockfronts can be calculated analytically in the planar approximation using the Rankine-Hugoniot-Taub adiabat (RHTA)[59]

$$\frac{w_1^2}{\rho_1^2} - \frac{w_2^2}{\rho_2^2} + (p_2 - p_1) \left(\frac{w_1}{\rho_1^2} + \frac{w_2}{\rho_2^2} \right) = 0 \quad , \quad (10)$$

where $w = e + p$ denotes the enthalpy, ρ the particle density, and p the pressure in the medium in front (1) and behind (2) the relativistic shockfront.

Fig. 5 shows shock waves calculated from Eq. (10) with different energy densities $\epsilon_2 = 40, 100, 200$ and 400 GeV/fm³ that travel through the ”normal”, heavy ion induced quark-gluon plasma which is assumed to have an energy density of $\epsilon_1 = 20$ GeV/fm³. The isentropes (full lines) lead to the respective freeze-out points using a hadronization criterion of $\epsilon = 1$ GeV/fm³. Note that the jet-induced shocks create considerable entropy. This leads to a strong shift of the hadronization density and baryochemical potential per quark, μ_q , to lower values.

Now, a Heckler-Kapusta-Hawking plasma with an initial temperature of 500 GeV can explode into the quark-gluon plasma with a temperature of ~ 500 MeV. As mentioned above, this hot HKH plasma contains besides the different quarks and leptons also photons, electrons, myons, tauons, $W^{+/-}$ and Z bosons, whereas the quark-gluon plasma created during the heavy ion collision is formed by quarks and gluons. Therefore, additional conservation laws have to be taken into account at the shock front [62]. The characteristics of the jet-induced hydrodynamic shocks is analogous to Fig. 5. However, the hadronization chemical potential is ignorable small for all practical purposes. Hence, exact particle-antiparticle symmetry should prevail, just as in the early universe.

Mach shocks can also occur if the HKH plasma is not created, but instead mono-jets from black holes (formed in Pb-Pb collisions at the LHC) induce Mach-waves travelling through the quark-gluon plasma, as calculated in Fig. 10. They can easily be observed, as at RHIC, by the two- and three- particle correlation functions, at Mach angles given by the well-known Mach relation $\phi = \arccos(v_s/v_{jet})$, where ϕ is the emission angle of the Mach shock particles relative to the jet axis.

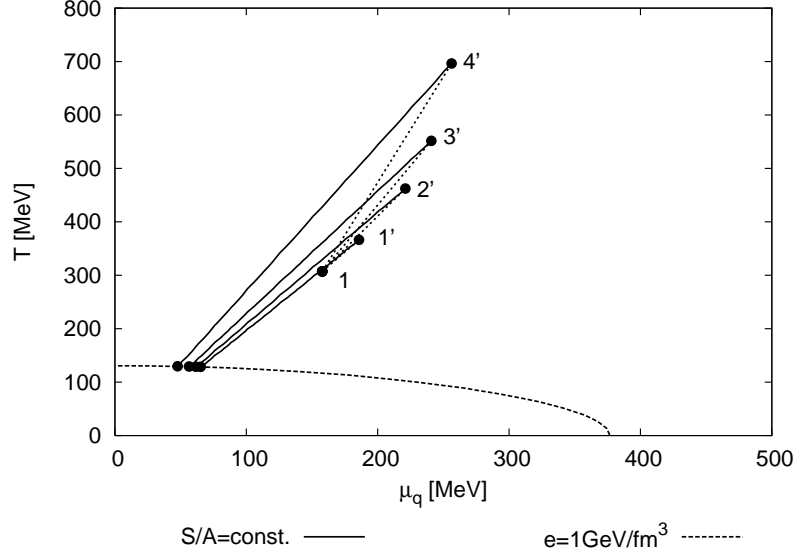


Fig. 5. Jet-induced secondary hydrodynamic shocks travelling through the baryon-rich QGP (1) with $\epsilon_1 = 20 \text{ GeV/fm}^3$, $\rho_1 = 2 \text{ fm}^{-3}$, $S/A = 41$. Four different e_2 -values are adopted: (1') $\epsilon_2 = 40 \text{ GeV/fm}^3$, $S/A = 41.6$, (2') $\epsilon_2 = 100 \text{ GeV/fm}^3$, $S/A = 44$, (3') $\epsilon_2 = 200 \text{ GeV/fm}^3$, $S/A = 48.1$, (4') $\epsilon_2 = 500 \text{ GeV/fm}^3$, $S/A = 57$.

A final word to the propagation of a possible black hole remnant (BHR) through the quark-gluon plasma: the average momentum of such a BHR is huge (several hundred GeV), and despite the expected mass $M_{\text{BHR}} = M_f = 1 \text{ TeV}$, the typical BHR-velocity moving through the quark-gluon plasma is calculated to be about $v_{\text{BHR}} \sim 0.9c$, at least for the lightest black holes. Hence, BHR-induced Mach cones may be caused by the relative flow of the Pb-Pb QCD plasma relative to the BHR can occur for either

- fast BHRs with velocity $v_{\text{BHR}} \gg c_{\text{QGP}} = 0.57c$, which are produced at the center of the QGP, where the flow of the plasma relative to the center-of-mass frame is negligible or
- slower BHRs which are created in the periphery of the Pb-Pb corona, but move "inwards", against the strong outward flow of the Pb-Pb QCD-plasma, for which the expected average outward "radial" flow velocities may considerably exceed $c_s \sim 0.57c$.

8. Conclusion

The LHC will provide exciting discovery potential way beyond supersymmetric extensions of the Standard Model. We have shown the different aspects of black hole formation and decay on microscopic scales and have discussed experimental signatures. In particular, we predict a complete suppression of back-to-back correlated di-jets, independent of the specific scenario. We have discussed the possibility of the formation of stable black hole remnants and have shown how signatures in the ALICE TPC chamber can be used to discriminate between complete decay and remnant formation. We also examine the possibility of the formation and expansion of a Heckler-Kapusta-Hawking plasma outside the horizon of the black hole. Without such a plasma, hard mono-jets from black hole decay would be observed in the detector; with such a plasma, those mono-jets will be absorbed and replaced by a high number of energetic particles expanding in a blast wave. In the case of black hole formation in a heavy ion collision, additional effects are observable due to the interaction of the black hole products with the surrounding bulk quark-gluon plasma. In particular, Mach shocks in the QGP may be caused by either the blast wave from the HKH plasma or by hard mono-jets from black hole decay or by fast moving black hole remnants.

Acknowledgements

This work has been supported by GSI, BMBF and the ALICE collaboration.

Discussions with and important contributions by the following colleagues are acknowledged:

Harry Appelshäuser, Peter Braun-Munzinger, Adrian Dumitru, Sabine Hossfelder, Kerstin Paech and Gebhard Zeeb.

References

1. K. Schwarzschild, Sitzungsberichte der Deutschen Akademie der Wissenschaften zu Berlin, Klasse für Mathematik, Physik und Technik, 189 (1916)
2. I. Antoniadis, Phys. Lett. B **246**, 377 (1990); I. Antoniadis and M. Quiros, Phys. Lett. B **392**, 61 (1997) [arXiv:hep-th/9609209]; K. R. Dienes, E. Dudas and T. Gherghetta, Nucl. Phys. B **537**, 47 (1999) [arXiv:hep-ph/9806292]; K. R. Dienes, E. Dudas and T. Gherghetta, Phys. Lett. B **436**, 55 (1998) [arXiv:hep-ph/9803466].
3. N. Arkani-Hamed, S. Dimopoulos and G. R. Dvali, Phys. Lett. B **429**, 263 (1998) [arXiv:hep-ph/9803315]; I. Antoniadis, N. Arkani-Hamed, S. Dimopoulos and G. R. Dvali, Phys. Lett. B **436**, 257 (1998) [arXiv:hep-ph/9804398]; N. Arkani-Hamed, S. Dimopoulos and G. R. Dvali, Phys. Rev. D **59**, 086004 (1999) [arXiv:hep-ph/9807344].

4. L. Randall and R. Sundrum, Phys. Rev. Lett. **83**, 4690 (1999) [arXiv:hep-th/9906064]; Phys. Rev. Lett. **83**, 3370 (1999) [arXiv:hep-ph/9905221].
5. K. Cheung [arXiv:hep-ph/0409028]; G. Landsberg [CDF and D0 - Run II Collaboration] [arXiv:hep-ex/0412028].
6. T. Banks and W. Fischler [arXiv:hep-th/9906038].
7. S. Dimopoulos and G. Landsberg, Phys. Rev. Lett. **87**, 161602 (2001) [arXiv:hep-ph/0106295]; P.C. Argyres, S. Dimopoulos, and J. March-Russell, Phys. Lett. B **441**, 96 (1998) [arXiv:hep-th/9808138].
8. R. Emparan, G. T. Horowitz and R. C. Myers, Phys. Rev. Lett. **85**, 499 (2000).
9. S. B. Giddings and S. Thomas, Phys. Rev. D **65** 056010 (2002) [hep-ph/0106219].
10. K. M. Cheung, Phys. Rev. Lett. **88**, 221602 (2002) [arXiv:hep-ph/01110163]; Y. Uehara [arXiv:hep-ph/0205068]; Y. Uehara, Prog. Theor. Phys. **107**, 621 (2002) [arXiv:hep-ph/0110382]; L. Anchordoqui and H. Goldberg, Phys. Rev. D **67**, 064010 (2003) [arXiv:hep-ph/0209337].
11. S. Hossenfelder, S. Hofmann, M. Bleicher and H. Stöcker, Phys. Rev. D **66**, 101502 (2002) [arXiv:hep-ph/0109085].
12. S. Hossenfelder, M. Bleicher, S. Hofmann, J. Ruppert, S. Scherer and H. Stöcker, Phys. Lett. B **575**, 85 (2003) [arXiv:hep-th/0305262].
13. S. Hossenfelder, M. Bleicher, S. Hofmann, H. Stöcker and A. V. Kotwal, Phys. Lett. B **566**, 233 (2003) [arXiv:hep-ph/0302247].
14. R. Casadio and B. Harms, Phys. Rev. D **64**, 024016 (2001) [arXiv:hep-th/0101154].
15. S. Alexeyev, A. Barrau, G. Boudoul, O. Khovanskaya and M. Sazhin, Class. Quant. Grav. **19**, 4431 (2002) [arXiv:gr-qc/0201069].
16. J. Alvarez-Muniz, J. L. Feng, F. Halzen, T. Han and D. Hooper, Phys. Rev. D **65**, 124015 (2002) [arXiv:hep-ph/0202081]; I. Mocioiu, Y. Nara and I. Sarcevic, Phys. Lett. B **557**, 87 (2003) [arXiv:hep-ph/0301073]; M. Cavaglia, S. Das and R. Maartens, Class. Quant. Grav. **20**, L205 (2003); [arXiv:hep-ph/0305223]; M. Cavaglia and S. Das, Class. Quant. Grav. **21**, 4511 (2004) [arXiv:hep-th/0404050].
17. A. Chamblin and G. C. Nayak, Phys. Rev. D **66**, 091901 (2002) [arXiv:hep-ph/0206060].
18. A. Casanova and E. Spallucci, Class. Quant. Grav. **23**, R45 (2006) [arXiv:hep-ph/0512063].
19. S. Hofmann, M. Bleicher, L. Gerland, S. Hossenfelder, K. Paech and H. Stöcker, J. Phys. G **28**, 1657 (2002); S. Hofmann, M. Bleicher, L. Gerland, S. Hossenfelder, S. Schwabe and H. Stöcker [arXiv:hep-ph/0111052]. Phys. Lett. **548**, 73 (2002).
20. R. Casadio and B. Harms, Int. J. Mod. Phys. A **17**, 4635 (2002) [arXiv:hep-th/0110255]; I. Ya. Yref'eva, Part.Nucl. 31, 169-180 (2000) [hep-th/9910269]; S. B. Giddings and V. S. Rychkov, Phys. Rev. D **70**, 104026 (2004) [arXiv:hep-th/0409131]; V. S. Rychkov [arXiv:hep-th/0410041];

- T. Banks and W. Fischler [arXiv:hep-th/9906038]; O. V. Kancheli [arXiv:hep-ph/0208021].
21. S. Hossenfelder, Phys. Lett. B **598**, 92 (2004) [arXiv:hep-th/0404232].
 22. S. Hossenfelder [arXiv:hep-ph/0510236].
 23. H. Stöcker, Int. J. Mod. Phys. D, (2006) [arXiv:hep-ph/0605062].
 24. H. Stöcker, to be published in Journal of Physics G (2006).
 25. G. L. Alberghi, R. Casadio, D. Galli, D. Gregori, A. Tronconi and V. Vagnoni [arXiv:hep-ph/0601243].
 26. A. Goyal, A. Gupta and N. Mahajan, Phys. Rev. D **63**, 043003 (2001) [arXiv:hep-ph/0005030]; R. Emparan, M. Masip and R. Rattazzi, Phys. Rev. D **65**, 064023 (2002) [arXiv:hep-ph/0109287]; D. Kazanas and A. Nicolaidis, Gen. Rel. Grav. **35**, 1117 (2003) [arXiv:hep-ph/0109247].
 27. A. Ringwald and H. Tu, Phys. Lett. B **525** 135-142 (2002) [arXiv:hep-ph/0111042]; J. Feng and A. Shapere, Phys. Rev. Lett. **88**, 021303 (2002); A. Cafarella, C. Coriano and T. N. Tomaras [arXiv:hep-ph/0410358]; L. A. Anchordoqui, J. L. Feng, H. Goldberg and A. D. Shapere, Phys. Rev. D **65** 124027 (2002) [arXiv:hep-ph/0112247]; S. I. Dutta, M. H. Reno and I. Sarcevic, Phys. Rev. D **66**, 033002 (2002) [arXiv:hep-ph/0204218]; U. Harbach and M. Bleicher [arXiv:hep-ph/0601121]; E. J. Ahn, M. Ave, M. Cavaglia and A. V. Olinto, Phys. Rev. D **68**, 043004 (2003).
 28. R. C. Myers and M. J. Perry, Ann. Phys. **172**, 304-347 (1986).
 29. K. S. Thorne, in Klauder, J., ed., Magic without Magic, 231-258, (W. H. Freeman, San Francisco, 1972).
 30. M. B. Voloshin, Phys. Lett. B **518**, 137 (2001) [arXiv:hep-ph/0107119]; Phys. Lett. B **524**, 376 (2002) [arXiv:hep-ph/0111099]; S. B. Giddings, in *Proc. of the APS/DPF/DPB Summer Study on the Future of Particle Physics (Snowmass 2001)* ed. N. Graf, eConf **C010630**, P328 (2001) [arXiv:hep-ph/0110127].
 31. V. S. Rychkov, Phys. Rev. D **70**, 044003 (2004) [arXiv:hep-ph/0401116]; K. Kang and H. Nastase [arXiv:hep-th/0409099].
 32. A. Jevicki and J. Thaler, Phys. Rev. D **66**, 024041 (2002); T. G. Rizzo, in *Proc. of the APS/DPF/DPB Summer Study on the Future of Particle Physics (Snowmass 2001)* ed. N. Graf, eConf **C010630**, P339 (2001); T. G. Rizzo [arXiv:hep-ph/0601029]; D. M. Eardley and S. B. Giddings, Phys. Rev. D **66**, 044011 (2002) [arXiv:gr-qc/0201034]; T. G. Rizzo [arXiv:hep-ph/0606051].
 33. H. Yoshino and Y. Nambu, Phys. Rev. D **67**, 024009 (2003) [arXiv:gr-qc/0209003].
 34. S. N. Solodukhin, Phys. Lett. B **533**, 153-161 (2002) [hep-ph/0201248]; D. Ida, K. Y. Oda and S. C. Park, Phys. Rev. D **67**, 064025 (2003) [Erratum-ibid. D **69**, 049901 (2004)] [arXiv:hep-th/0212108].
 35. G. T. Horowitz and J. Polchinski, Phys. Rev. D **66**, 103512 (2002) [arXiv:hep-th/0206228].
 36. G. Landsberg, [arXiv:hep-ph/0211043]; M. Cavaglia, Int. J. Mod. Phys. A **18**, 1843 (2003) [arXiv:hep-ph/0210296]; S. Hossenfelder, [arXiv:hep-ph/0412265].
 37. M. Bleicher, S. Hofmann, S. Hossenfelder and H. Stöcker, Phys. Lett. B **548**,

- 73 (2002).
38. A. Chamblin, F. Cooper and G. C. Nayak, Phys. Rev. D **69**, 065010 (2004) [arXiv:hep-ph/0301239].
 39. L. Lonnblad, M. Sjoedahl and T. Akesson [arXiv:hep-ph/0505181].
 40. S. W. Hawking, Comm. Math. Phys. **43**, 199-220 (1975); Phys. Rev. D **14**, 2460-2473 (1976).
 41. S. Hossenfelder, B. Koch and M. Bleicher [arXiv:hep-ph/0507140].
 42. P. Kanti, Int. J. Mod. Phys. A **19**, 4899 (2004).
 43. D. N. Page, Phys. Rev. D **13**, 198 (1976); R. Casadio and B. Harms, Phys. Lett. **B 487**, 209-214 (2000) [arXiv:hep-th/0004004].
 44. P. Kraus and F. Wilczek, Nucl. Phys. B **433**, 403 (1995) [arXiv:gr-qc/9408003]; P. Kraus and F. Wilczek, Nucl. Phys. B **437**, 231 (1995) [arXiv:hep-th/9411219]; E. Keski-Vakkuri and P. Kraus, Nucl. Phys. B **491**, 249 (1997) [arXiv:hep-th/9610045]; S. Massar and R. Parentani, Nucl. Phys. B **575**, 333 (2000) [arXiv:gr-qc/9903027]; T. Jacobson and R. Parentani, Found. Phys. **33**, 323 (2003) [arXiv:gr-qc/0302099]; M. K. Parikh and F. Wilczek, Phys. Rev. Lett. **85**, 5042 (2000) [arXiv:hep-th/9907001].
 45. A. Bonanno and M. Reuter, Phys. Rev. D **62**, 043008 (2000) [arXiv:hep-th/0002196]; R. J. Adler, P. Chen and D. I. Santiago, Gen. Rel. Grav. **33**, 2101 (2001) [arXiv:gr-qc/0106080]; T. G. Rizzo, [arXiv:hep-ph/0510420]; T. G. Rizzo, [arXiv:hep-ph/0601029]; A. Bonanno and M. Reuter [arXiv:hep-th/0602159]; K. Nozari and B. Fazlpour, [arXiv:hep-th/0605109].
 46. R. G. Daghigh and J. I. Kapusta, Phys. Rev. D **65**, 064028 (2002) [arXiv:gr-qc/0109090].
 47. R. Barbera, B. Batyunya, Yu. Belikov, M. Botje, P. G. Cerello, A. Feliciello, T. Humanic, G. Lo Curto, A. Palmeri, F. Riggi, ALICE Internal Note ALICE/ITS 98-06; T. J. Humanic, ALICE note: ALICE-INT-2005-017; T. Humanic, B. Koch and H. Stöcker, accepted for publication in Int. J. Mod. Phys. E (2006).
 48. T. Sjostrand, L. Lonnblad and S. Mrenna [arXiv:hep-ph/0108264].
 49. C. M. Harris, P. Richardson and B. R. Webber, JHEP **0308**, 033 (2003); [arXiv:hep-ph/0307305].
 50. J. Tanaka, T. Yamamura, S. Asai and J. Kanzaki [arXiv:hep-ph/0411095].
 51. C. M. Harris, M. J. Palmer, M. A. Parker, P. Richardson, A. Sabetfakhri and B. R. Webber [arXiv:hep-ph/0411022].
 52. B. Koch, M. Bleicher and S. Hossenfelder, JHEP **0510**, 053 (2005) [arXiv:hep-ph/0507138].
 53. P. Cortese *et al.* [ALICE Collaboration], CERN-LHCC-2002-016.
 54. A. F. Heckler, Phys. Rev. D **55**, 480 (1997) [arXiv:astro-ph/9601029]; Phys. Rev. Lett. **78**, 3430 (1997) [arXiv:astro-ph/9702027].
 55. J. I. Kapusta, Phys. Rev. Lett. **86**, 1670-1673 (2001).
 56. L. P. Csernai, B. Lukacs and J. Zimanyi, Lett. Nuovo Cim. **27** 111 (1980).
 57. P. J. Siemens and J. O. Rasmussen, Phys. Rev. Lett. **42**, 880 (1979).

-
58. H. Stöcker, A. A. Ogloblin and W. Greiner, *Z. Phys. A* **303**, 259 (1981).
 59. J. Hofmann, H. Stöcker, W. Scheid and G. W., *Report of the Workshop on BeV/nucleon Collisions of Heavy Ions: How and Why, Bear Mountain, New York, 29 Nov - 1 Dec 1974*; H. G. Baumgardt *et al.*, *Z. Phys. A* **273**, 359 (1975); J. Hofmann, H. Stöcker, U. W. Heinz, W. Scheid and W. Greiner, *Phys. Rev. Lett.* **36**, 88 (1976); H. Stöcker, J. Hofmann, J. A. Maruhn and W. Greiner, *Prog. Part. Nucl. Phys.* **4**, 133 (1980); H. Stöcker, J. A. Maruhn and W. Greiner, *Phys. Rev. Lett.* **44**, 725 (1980); H. Stöcker, G. Graebner, J. A. Maruhn and W. Greiner, *Phys. Lett. B* **95**, 192 (1980); H. Stöcker and W. Greiner, *Phys. Rept.* **137**, 277 (1986); G.F. Chapline and A. Granik, *Nucl. Phys. A* **459**, 681 (1986); D.H. Rischke, H. Stöcker and W. Greiner, *Phys. Rev. D* **42**, 2283 (1990); J. Casalderrey–Solana, E.V. Shuryak and D. Teaney, [arXiv:hep-ph/0411315]; E.V. Shuryak, talk at Int. Conf. Quark Matter 2005, Budapest, Hungary, 2005.
 60. H. Stöcker, *Nucl. Phys. A* **750**, 121 (2005) [arXiv:nucl-th/0406018].
 61. L. M. Satarov, H. Stöcker and I. N. Mishustin, *Phys. Lett. B* **627**, 64 (2005) [arXiv:hep-ph/0505245].
 62. B. Betz et al., to be published.